RESEARCH ARTICLE

Association of Seizure Foci and Location of Tau and Amyloid Deposition and Brain Atrophy in Patients With Alzheimer Disease and Seizures

Alice D. Lam, MD, PhD, Emma G. Thibault, BS, Danielle V. Mayblyum, BS, Stephanie Hsieh, BS, Kyle R. Pellerin, BA, Eliezer J. Sternberg, MD, Anand Viswanathan, MD, PhD, Stephanie Buss, MD, Rani A. Sarkis, MD, MSc, Heidi I.L. Jacobs, PhD, Keith A. Johnson, MD, and Reisa A. Sperling, MD

Correspondence
Dr. Lam
lam.alice@mgh.harvard.edu

Neurology® 2024;103:e209920. doi:10.1212/WNL.0000000000209920

Abstract

Background and Objectives

Alzheimer disease (AD) is associated with a 2 to 3-fold increased risk of developing late-onset focal epilepsy, yet it remains unclear how development of focal epilepsy in AD is related to AD pathology. The objective of this study was to examine spatial relationships between the epileptogenic zone and tau deposition, amyloid deposition, and brain atrophy in individuals with AD who developed late-onset, otherwise unexplained focal epilepsy. We hypothesized that if network hyperexcitability is mechanistically linked to AD pathology, then there would be increased tau and amyloid deposition within the epileptogenic hemisphere.

Methods

In this cross-sectional study, we performed tau and amyloid PET imaging, brain MRI, and overnight scalp EEG in individuals with early clinical stages of AD who developed late-onset, otherwise unexplained focal epilepsy (AD-Ep). Participants were referred from epilepsy and memory disorders clinics at our institutions. We determined epilepsy localization based on EEG findings and seizure semiology. We quantified tau deposition, amyloid deposition, and atrophy across brain regions and calculated asymmetry indices for these measures. We compared findings in AD-Ep with those in a control AD group without epilepsy (AD-NoEp).

Results

The AD-Ep group included 8 individuals with a mean age of 69.5 ± 4.2 years at PET imaging. The AD-NoEp group included 14 individuals with a mean age of 71.7 ± 9.8 years at PET imaging. In AD-Ep, we found a highly asymmetric pattern of tau deposition, with significantly greater tau in the epileptogenic hemisphere. Amyloid deposition and cortical atrophy were also greater in the epileptogenic hemisphere, although the magnitudes of asymmetry were reduced compared with tau. Compared with AD-NoEp, the AD-Ep group had significantly greater tau asymmetry and trends toward greater asymmetry of amyloid and atrophy. AD-Ep also had significantly greater amyloid burden bilaterally and trends toward greater tau burden within the epileptogenic hemisphere, compared with AD-NoEp.

Discussion

Our results reveal a spatial association between the epileptogenic focus and tau deposition, amyloid deposition, and neurodegeneration in early clinical stages of AD. Within the limitations of a cross-sectional study with small sample sizes, these findings contribute to our understanding of the clinicopathologic heterogeneity of AD, demonstrating an association between focal epilepsy and lateralized pathology in AD.

From the Department of Neurology (A.D.L., S.H., K.R.P., A.V., K.A.J.), Massachusetts General Hospital, Boston; Harvard Medical School (A.D.L., A.V., S.B., R.A. Sarkis, H.L.J., K.A.J., R.A. Sperling), Boston; Department of Radiology (E.G.T., D.V.M., H.L.J., K.A.J.), Massachusetts General Hospital, Boston; Department of Neurology (E.J.S.), Milford Regional Medical Center; Department of Neurology (S.B.), Beth Israel Deaconess Medical Center, Boston; and Department of Neurology (R.A.Sarkis, R.A.Sperling), Brigham and Women's Hospital, Boston, MA.

Go to Neurology.org/N for full disclosures. Funding information and disclosures deemed relevant by the authors, if any, are provided at the end of the article.

Glossary

AI = asymmetry index; **CDR** = Clinical Dementia Rating; **DVR** = distribution volume ratio; **FDR** = false discovery rate; **MCI** = mild cognitive impairment; **PIB** = Pittsburgh Compound B; **PVC** = partial volume correction; **ROIs** = regions of interest; **SUVR** = standardized uptake value ratio.

Introduction

Network hyperexcitability has emerged as an important contributor to cognitive dysfunction and clinical progression in Alzheimer disease (AD).[1,2] Individuals with AD carry a 2 to 3-fold increased risk of developing seizures compared with their healthy peers,[3] and those who develop AD-related epilepsy present with cognitive decline up to 5 years earlier than those who do not develop epilepsy.[4] This suggests that neuronal hyperexcitability could play an important role in accelerating preclinical and early clinical stages of AD. Genetic mouse models of AD have consistently revealed a feed-forward cycle that directly links neuronal hyperactivity with excess release of soluble amyloid and tau and with subsequent deposition of these proteins as insoluble plaques and tangles, respectively.[5-8] Moreover, increasing evidence indicates that tau pathology propagates trans-synaptically across neuronal networks.[9-11] Whether and how the development of epilepsy in human AD is associated with amyloid or tau pathology remains unclear.

In this article, we studied 8 individuals with early clinical stages of AD who developed epilepsy early in their course of AD. All individuals underwent PET imaging to visualize tau and amyloid deposition in vivo. A consistent feature of epilepsy in human AD is that it is most often focal, arising from a unilateral temporal lobe.[12,13] We hypothesized that if neuronal hyperexcitability in AD is mechanistically linked to accumulation of AD pathology, then unilateral temporal lobe hyperexcitability in individuals with AD and epilepsy will be accompanied by asymmetric, focally increased deposition of tau and/or amyloid within the epileptogenic hemisphere.

Methods

Standard Protocol Approvals, Registrations, and Patient Consents

All research was performed under protocols approved by the MassGeneral Brigham Institutional Review Board (Protocols #2018P000286, 2018P000821). All research participants provided written informed consent before their participation.

Participant Recruitment

AD With Epilepsy (AD-Ep) Group

We previously described AD-Ep participant 1, in whom intracranial foramen ovale electrode recordings revealed silent hippocampal seizures and spikes.[14] This participant underwent PET imaging as part of a separate research study. The remaining 7 participants were consecutively recruited for this study, through outpatient epilepsy and memory disorders clinics at our institutions, between 2019 and 2022. Inclusion criteria were the following: (1) age 60–85 years; (2) early clinical stages of probable AD (either mild cognitive impairment (MCI) or mild dementia), based on the National Institute of Aging-Alzheimer's Association criteria[15,16]; and (3) diagnosis of epilepsy based on International League Against Epilepsy criteria,[17] with seizures starting after age 55 and etiology otherwise unexplained (e.g., lack of epileptogenic brain lesions such as stroke or tumor and lack of other convincing etiologies for epilepsy outside of AD). Exclusion criteria included a history of stroke, traumatic brain injury with loss of consciousness, meningitis/encephalitis, brain tumor, or brain surgery preceding the diagnosis of epilepsy (i.e., intracranial electrode recordings performed for clinical indication of epilepsy were not exclusionary).

AD Control Group Without Epilepsy (AD-NoEp Group)

Data for this group were obtained from a separate PET imaging study performed at Massachusetts General Hospital. Inclusion criteria for this PET imaging study were as follows: (1) age 46–100 years; (2) clinical diagnosis of MCI or AD by a neurologist, using NIH consensus criteria; (3) Clinical Dementia Rating (CDR) score ≥0.5; and (4) stable medications for at least 30 days. Exclusion criteria included the following: seizure disorder; presence of a significant medical, neurologic, or psychiatric disorder other than diagnosis of MCI or AD (not including mild depression); and presence of another neurodegenerative disease associated with cognitive impairment or dementia. The AD-NoEp group comprised a subset of participants from this study who were amyloid positive, based on Pittsburgh Compound B (PIB) PET imaging.

Neurophysiologic Recordings

All AD-Ep participants underwent overnight ambulatory scalp EEG recordings for research as described previously.[13] We also examined EEGs and, in some cases, intracranial electrode recordings performed for clinical purposes. Designation of the most likely epileptogenic focus for each participant was made by board-certified epileptologists (ADL, RAS, ES) based on neurophysiologic recordings and seizure semiology.

Structural MRI

High-resolution T1-weighted images were acquired on either a Siemens 3T Skyra scanner (AD-Ep participant 6) or a Siemens 3T Tim Trio scanner (all other participants), using a magnetization-prepared rapid gradient-echo sequence. Images were processed with FreeSurfer 6[18,19] and parcellated into cortical and subcortical regions of interest (ROIs) according to the Desikan-Killiany atlas.[20] Segmentation results were manually checked to ensure accuracy.

PET Imaging

Radiotracers were synthesized at Massachusetts General Hospital, and PET imaging was performed on site. AD-Ep participant 1 was imaged using Siemens/CTI ECAT EXACT HR+ while all others were imaged using a GE Discovery MI PET/CT scanner. All participants underwent amyloid imaging with ^{11}C PIB and tau imaging with ^{18}F-flortaucipir (FTP, AD-Ep participant 1) or ^{18}F-MK-6240 (all other participants). PIB: Participants were given a 15-mCi bolus injection, followed by a 60-minute dynamic acquisition in 39 frames (8 × 15 seconds, 4 × 60 seconds, 27 × 120 seconds). FTP: AD-Ep participant 1 was given a 10-mCi bolus injection, followed by image acquisition from 80 to 100 minutes after injection, in 4 × 5-minute frames. MK-6240: Participants were given a 5-mCi bolus injection, followed by a 120-minute dynamic acquisition in 54 frames (6 × 10 seconds, 8 × 15 seconds, 6 × 30 seconds, 8 × 60 seconds, 8 × 120 seconds, 18 × 300 seconds).

PET images were reconstructed, attenuation corrected, and co-registered to T1 images with SPM12, using a 6-degree-of-freedom rigid-body registration. Structural ROIs from FreeSurfer 6 were mapped into native PET space. PIB data were expressed as a distribution volume ratio (DVR) for each ROI, using the Logan graphical method[21] applied to data from 40 to 60 minutes after injection. FTP and MK-6240 data were expressed as a standardized uptake value ratio (SUVR) for each ROI and calculated from PET data acquired 80–100 and 90–110 minutes after injection, respectively. Cerebellar gray was used as the reference for all analyses. Partial volume correction (PVC) was performed using the GTM method, and analyses were performed with and without PVC.

Global amyloid burden on PIB PET was summarized using a FreeSurfer-defined aggregate ROI comprising the frontal, lateral temporal and parietal, and retrosplenial (FLR) cortices, as described previously.[22] An FLR SUVR (non-PVC) > 1.12 was considered a positive amyloid PET scan.

Asymmetry Index (AI) Calculations

We quantified tau, amyloid, and brain atrophy in cortical ROIs based on the Desikan-Killiany atlas, using FTP or MK-6240 SUVR, PIB DVR, or cortical thickness values, respectively. We also quantified these measures across 6 larger brain regions, by averaging values across multiple cortical ROIs, as performed previously[23,24]: (1) frontal (superior frontal, rostral and caudal middle frontal, lateral and medial orbitofrontal); (2) medial temporal (entorhinal, parahippocampal, hippocampus, amygdala; for cortical thickness measures, only entorhinal and parahippocampal regions were used); (3) lateral temporal (inferior, middle, and superior temporal, bank of superior temporal sulcus); (4) medial parietal (posterior cingulate, precuneus); (5) lateral parietal (inferior and superior parietal, supramarginal); and (6) occipital (pericalcarine, cuneus, lateral occipital).

To examine asymmetries in amyloid or tau deposition and their spatial relationship to the epileptogenic hemisphere in AD-Ep, we calculated an AI for each ROI as follows: 200 * (Ipsilateral - Contralateral)/(Ipsilateral + Contralateral), where ipsilateral and contralateral were DVR or SUVR values relative to the epileptogenic hemisphere. A positive AI indicates greater amyloid or tau deposition in the epileptogenic hemisphere. To ensure accuracy of AI calculations in ROIs with little tracer uptake, we set a threshold in which the DVR or SUVR of an ROI had to exceed 0.90 in both hemispheres for the AI to be calculated. We chose a slightly lower threshold because some AD-Ep participants had ROIs in which there was high tau accumulation in one hemisphere and background-level tau in the opposite hemisphere; thus, higher thresholds would have excluded these important findings from the analysis. AI for brain atrophy was calculated as 200 * (Contralateral - Ipsilateral)/(Ipsilateral + Contralateral). A positive AI indicates greater atrophy in the epileptogenic hemisphere.

We also compared asymmetry of amyloid, tau, and atrophy between AD-Ep and AD-NoEp groups. Because the AD-NoEp group does not have an epileptogenic hemisphere, here we calculated amyloid and tau asymmetry indices relative to the left hemisphere, as follows: 200 * (Left - Right)/(Left + Right), where a positive AI indicates greater amyloid or tau deposition in the left hemisphere. Similarly, AI for brain atrophy was calculated as follows: 200 * (Right - Left)/(Left + Right), where a positive AI indicates greater atrophy in the left hemisphere.

Statistical Analysis

Population statistics are given as mean ± SD. We used Mann-Whitney *U* tests for comparison of independent samples, Fisher exact tests for comparison of proportions, and Spearman correlations to measure associations.

Among AD-Ep participants, to identify ROIs in which AIs differed significantly from 0, we used right-tailed Mann-Whitney signed-rank tests. To compare magnitudes of tau, amyloid, and atrophy AIs between AD-Ep and AD-NoEp, we focused on AD-Ep participants with left-sided epilepsy and we used right-tailed Mann-Whitney *U* tests to determine whether AD-Ep participants with left-sided epilepsy showed significantly greater AIs (relative to the left hemisphere) than AD-NoEp. We did not perform this analysis for participants with right-sided epilepsy, given the lower sample size.

We accounted for multiple comparisons using the Benjamini and Hochberg method to control the false discovery rate (FDR). We report FDR-corrected p values (where, for right-tailed tests, an FDR-corrected $p < 0.025$ was considered statistically significant). Mann-Whitney standardized effect sizes (r) are also reported.

Data Availability

Data that support the findings of this study are available on reasonable request from the corresponding author.

Table 1 Clinical Details for AD-Ep Population

Participant	1	2	3	4	5	6	7	8
Handedness	Ambidextrous	Right	Left	Left	Right	Right	Left	Right
Age range at onset of cognitive decline (y)[a]	65–69	70–74	65–69	60–64	60–64	70–74	65–69	65–69
No. of years between cognitive decline and first seizure	0	+5	+1	+4	0	0	0	+1
No. of years between first seizure and PET imaging	+3	0	+2	0	+1	+3	+2	+2
Cognitive presentation	Amnestic	Amnestic	Amnestic	Amnestic	Amnestic	Amnestic	Amnestic	Amnestic
Epileptogenic region	L temporal (hippocampal)	L temporal	R temporal	L temporal	L temporoparietal	L temporal; later, R temporal	R temporal	R temporal
Clinical stage at PET imaging	Mild dementia	Mild dementia	MCI	Mild dementia	MCI	Mild dementia	MCI	Mild dementia
Amyloid PET tracer	PIB	PIB	PIB	PIB	PIB	PIB	PIB	PIB
Global PIB (FLR non-PVC)[b]	1.71	2.05	1.18	2.11	2.19	2.34	1.74	1.77
Tau PET tracer	FTP	MK6240	MK6240	MK6240	MK6240	MK6240	MK6240	MK6240

Abbreviations: MCI = mild cognitive impairment; PVC = partial volume correction.
[a] Identifiable details such as sex and exact ages are not provided, so as to protect participant privacy.
[b] FLR non-PVC > 1.12 indicates a positive PIB PET scan.

Results

AD-Ep Population Characteristics

We studied 8 individuals with early clinical stages of AD (MCI or mild dementia) who developed late-onset, otherwise unexplained focal epilepsy (AD-Ep). Demographic and clinical characteristics of the cohort are provided in Tables 1 and 2, and additional details are summarized in eTable 1. All participants had a predominantly amnestic presentation of AD. The average age at onset of cognitive decline was 66.5 ± 3.8 years and at first clinical seizure was 67.9 ± 4.0 years. Six participants had their first seizure in the same year that they developed cognitive impairments. Seven participants underwent CSF analysis for AD biomarkers; 6 had CSF-confirmed AD while 1 participant (participant 8) had borderline results due to low phospho-tau levels.

Four participants had exclusively nonconvulsive seizures while 2 had only convulsive seizures and 2 had nonconvulsive and convulsive seizures. EEG abnormalities for each participant are summarized in eTable 1, and examples of EEG findings from all participants are presented in eFigure 1. Five participants had left temporal lobe epilepsy, including 1 participant with left hippocampal seizures captured on intracranial electrodes. Three participants had right temporal lobe epilepsy.

Spatial Associations Between the Epileptogenic Focus and Tau, Amyloid, and Neurodegeneration

In all AD-Ep participants, we found a striking pattern of asymmetric tau deposition, with more tau deposited in the epileptogenic hemisphere (Figure 1A). Participants with higher global tau burden (AD-Ep participants 1–6) showed

Table 2 Comparison of AD-Ep and AD-NoEp Populations

	AD with epilepsy (AD-Ep)	AD without epilepsy (AD-NoEp)	*p* Value
Number of participants	8	14	—
Mean age at PET, y (range)	69.5 ± 4.2 (60–72)	71.7 ± 9.8 (58–84)	0.48
Percent female (#F/M)	62.5% (5/3)	35.7% (5/9)	0.38
Race (% White)	100%	100%	1.0
Ethnicity (% non-Hispanic)	100%	100%	1.0
Mean years of education	16.4 ± 2.6	16.4 ± 3.1	0.97
Mean PIB FLR DVR (no PVC)	1.89 ± 0.37	1.68 ± 0.36	0.21
MMSE (closest within 1 y of PET)	23.9 ± 3.4	22.8 ± 4.9	0.76

Figure 1 Representative Tau and Amyloid PET Images for AD-Ep Group

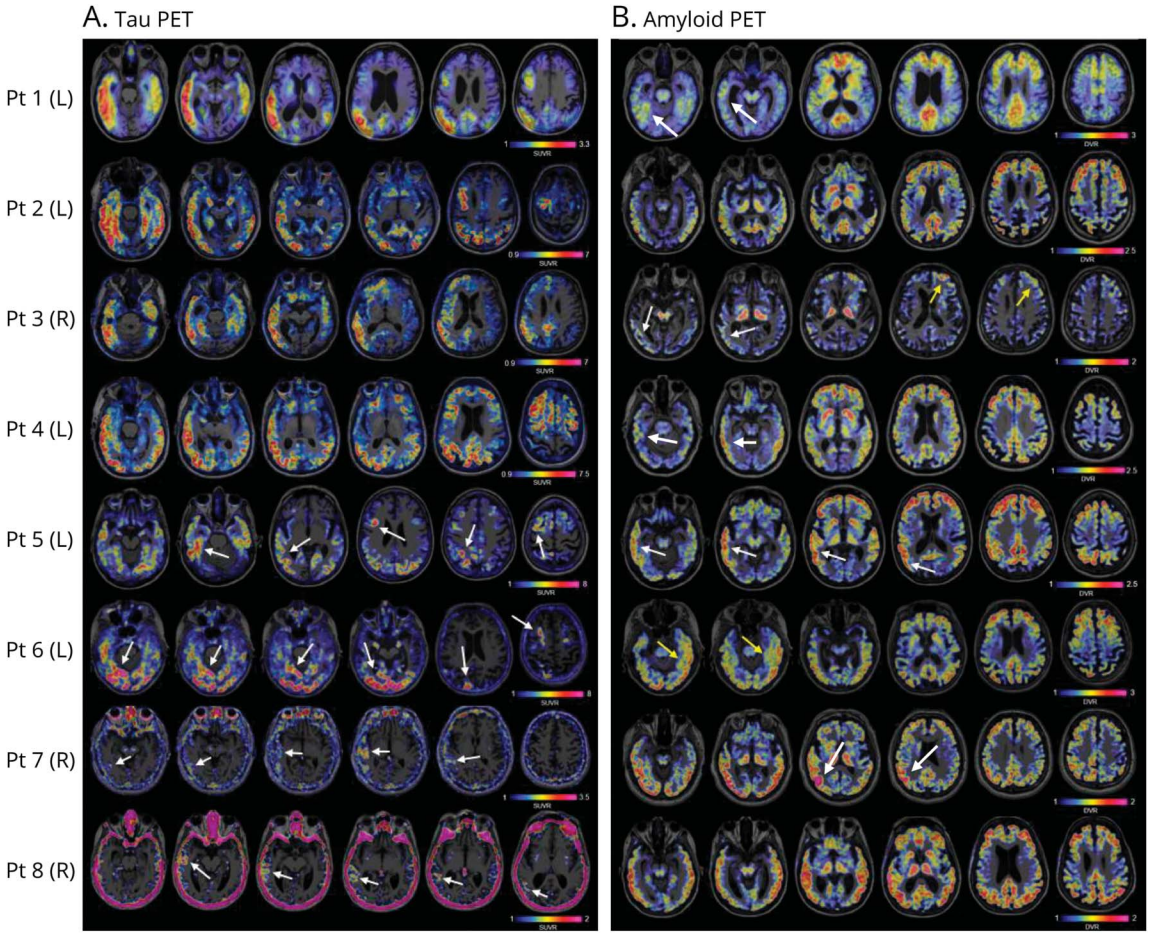

(A) Representative tau PET images. Axial slices are shown for each participant (Pt), arranged from inferior (left) to superior (right). Images are oriented such that the epileptogenic hemisphere for each participant is shown on the left. (L) and (R) indicate the epileptogenic hemisphere (left or right, respectively) for each participant. Participant 1 was imaged using ^{18}F-flortaucipir while participants 2–8 were imaged using ^{18}F-MK-6240. (B) Representative amyloid PET images. Image orientation is the same as for (A), and all participants were imaged using ^{11}C-PIB. White arrows highlight subtler regions of increased tau or amyloid deposition in the epileptogenic hemisphere while yellow arrows highlight increased amyloid in the contralateral hemisphere in some participants.

increased tau deposition broadly throughout the epileptogenic hemisphere while participants with lower global tau burden (AD-Ep participants 7–8) showed a highly focal accumulation of tau within the lateral temporal neocortex of the epileptogenic hemisphere. For most participants, tau deposition was highest in the temporal and parietal neocortex, although AD-Ep participant 6 was atypical, with most tau deposition in the occipital cortex but with high tau deposition in temporal and parietal regions as well.

We quantified tau asymmetry using an AI, calculated over 6 broad brain regions (Figure 2A) and within smaller cortical ROIs (eFigure 2). We found significantly higher tau deposition in the frontal (p = 0.023, r = 0.88), lateral temporal (p = 0.023, r = 0.94), medial parietal (p = 0.023, r = 0.88), and lateral parietal (p = 0.023, r = 0.91) regions of the epileptogenic hemisphere. These findings were evident both with and without PVC.

Compared with tau, patterns of amyloid asymmetry were subtler and more variable across participants (Figure 1B). Most AD-Ep participants showed areas of asymmetrically greater amyloid within the epileptogenic hemisphere, although the magnitude of this asymmetry was lower than for tau. Quantification of amyloid asymmetry (Figure 2B, eFigure 2) revealed significantly greater amyloid deposition in the lateral temporal (p = 0.011, r = 0.94), lateral parietal (p = 0.011, r = 0.94), and occipital (p = 0.023, r = 0.80) regions of the epileptogenic hemisphere, although these findings were only significant when PVC was used, possibly due to greater atrophy in the same regions (mentioned further). Two AD-Ep participants (participants 3 and 6) showed areas of increased amyloid deposition in the contralateral hemisphere (Figure 1B). Of interest, AD-Ep participant 6 had developed a secondary seizure focus in the contralateral hemisphere (presenting as focal status epilepticus) approximately 6 months before undergoing the amyloid PET scan.

We also examined patterns of cortical and subcortical atrophy in the AD-Ep group. We found increased atrophy within the epileptogenic hemisphere, although the magnitude of

Figure 2 Asymmetry Indices for Tau, Amyloid, and Cortical Atrophy in the AD-Ep Group

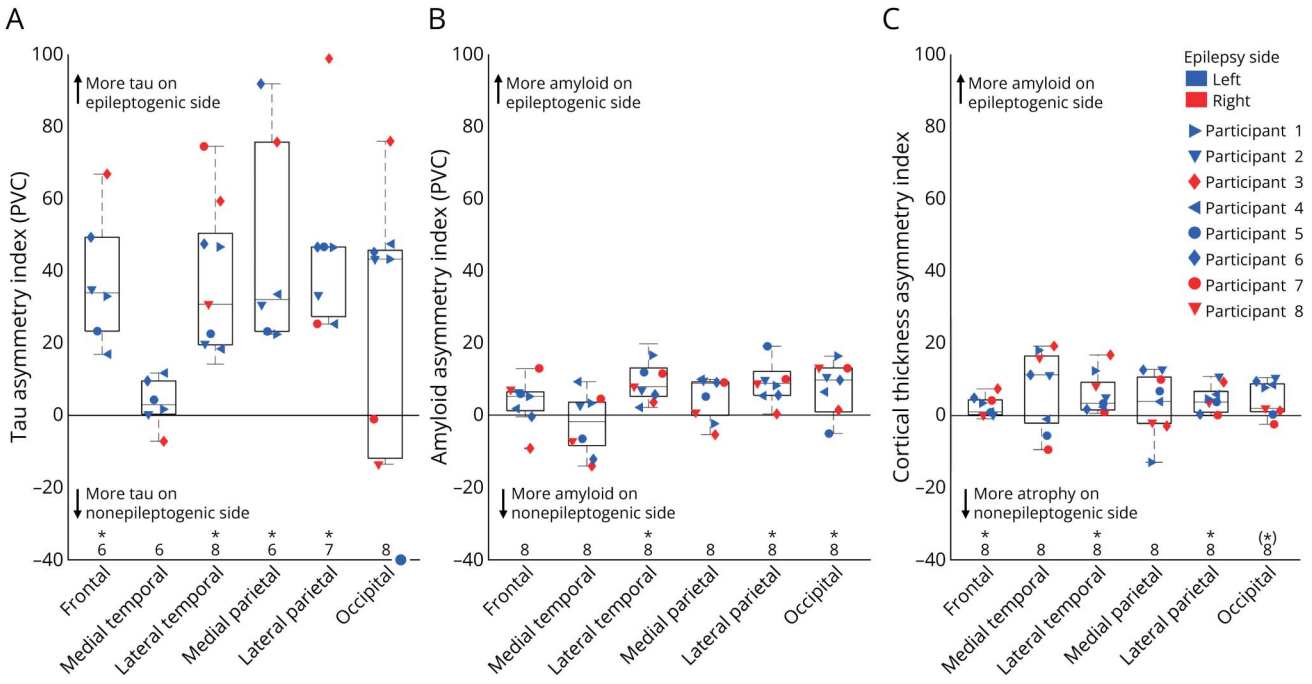

AIs were calculated with respect to the epileptogenic/nonepileptogenic hemisphere across 6 large brain regions, for (A) tau deposition, (B) amyloid deposition, and (C) cortical atrophy. A positive AI indicates greater tau deposition, amyloid deposition, or cortical atrophy in the epileptogenic hemisphere whereas a negative AI indicates greater tau deposition, amyloid deposition, or cortical atrophy in the nonepileptogenic hemisphere. Box-and-whisker plots for the AD-Ep population are shown, and individual AD-Ep participants are plotted as colored markers, based on whether their seizures arose from the left (blue) or right (red) hemisphere. AIs for tau and amyloid were calculated using partial volume–corrected SUVR and DVR values, respectively. Numbers above each ROI represent the number of participants in whom AIs could be calculated for that ROI (i.e., participants with above-threshold SUVR or DVR levels). Asterisks denote ROIs in which the AI was significantly different from 0 (FDR-corrected p value < 0.025), whereas asterisks in parentheses indicate trends toward significance. Note in part (A), on the occipital plot, participant 5 is plotted on the x-axis (blue filled circle at tau AI = −40), although this participant had a much larger magnitude of AI (> −100) that otherwise would not be seen due to the scaling of the plot (but can be seen in Figure 3A). AI = asymmetry index; DVR = distribution volume ratio; SUVR = standardized uptake value ratio.

asymmetry was much less than for tau. Quantification of cortical thickness asymmetry revealed significantly greater atrophy in the frontal (p = 0.008, r = 0.94), lateral temporal (p = 0.008, r = 0.94), and lateral parietal (p = 0.008, r = 0.94) regions and a trend toward greater atrophy in the occipital region (p = 0.041, r = 0.68) of the epileptogenic hemisphere (Figure 2C). Quantification of subcortical volume asymmetry revealed significantly greater atrophy in the amygdala (p = 0.023, r = 0.85), hippocampus (p = 0.023, r = 0.85), and nucleus accumbens (p = 0.023, r = 0.94) of the epileptogenic hemisphere (eFigure 3).

Comparison of Tau, Amyloid, and Atrophy Asymmetry Between AD-Ep and AD-NoEp Groups

We next compared asymmetry findings in the AD-Ep group with those in a control AD group without epilepsy (AD-NoEp). The AD-NoEp group comprised 14 individuals with early clinical stages of AD (MCI or mild dementia), no history of seizures, and amyloid positivity based on PIB PET imaging. Table 2 presents comparison of the demographic and clinical features of AD-Ep and AD-NoEp. There were no significant differences in age at PET scan, biological sex, MMSE score closest to PET scan, or global amyloid deposition between groups.

Figure 3 shows the tau, amyloid, and atrophy AIs for AD-Ep and AD-NoEp, calculated relative to the left hemisphere. In the AD-NoEp group, there were trends toward a rightward tau asymmetry in the medial temporal (p = 0.0425, r = 0.59), lateral parietal (p = 0.0425, r = 0.59), and occipital regions (p = 0.0425, r = 0.62), consistent with what has been reported previously.[25] In the AD-Ep group, tau AIs fell near or beyond the extremes of the distributions for the AD-NoEp group. In other words, most AD-Ep participants with left-sided epilepsy had tau AIs in or above the upper range of the AD-NoEp distribution (i.e., more leftward asymmetry compared with AD-NoEp), whereas those with right-sided epilepsy often showed tau AIs in or below the lower range of the AD-NoEp distribution (i.e., more rightward asymmetry compared with AD-NoEp). Quantitatively, AD-Ep participants with left-sided epilepsy had tau AIs that were significantly greater than in AD-NoEp in the medial parietal (p = 0.0210, r = 0.62) and lateral parietal (p = 0.0066, r = 0.68) regions and showed trends toward significance in the frontal (p = 0.0252, r = 0.58) and lateral temporal (p = 0.0252, r = 0.51) regions. We did not perform statistical testing for the AD-Ep group with right-sided epilepsy, given the low number of participants.

Figure 3 Comparison of Tau Asymmetry, Amyloid Asymmetry, and Atrophy Asymmetry Between AD-Ep and AD-NoEp Groups

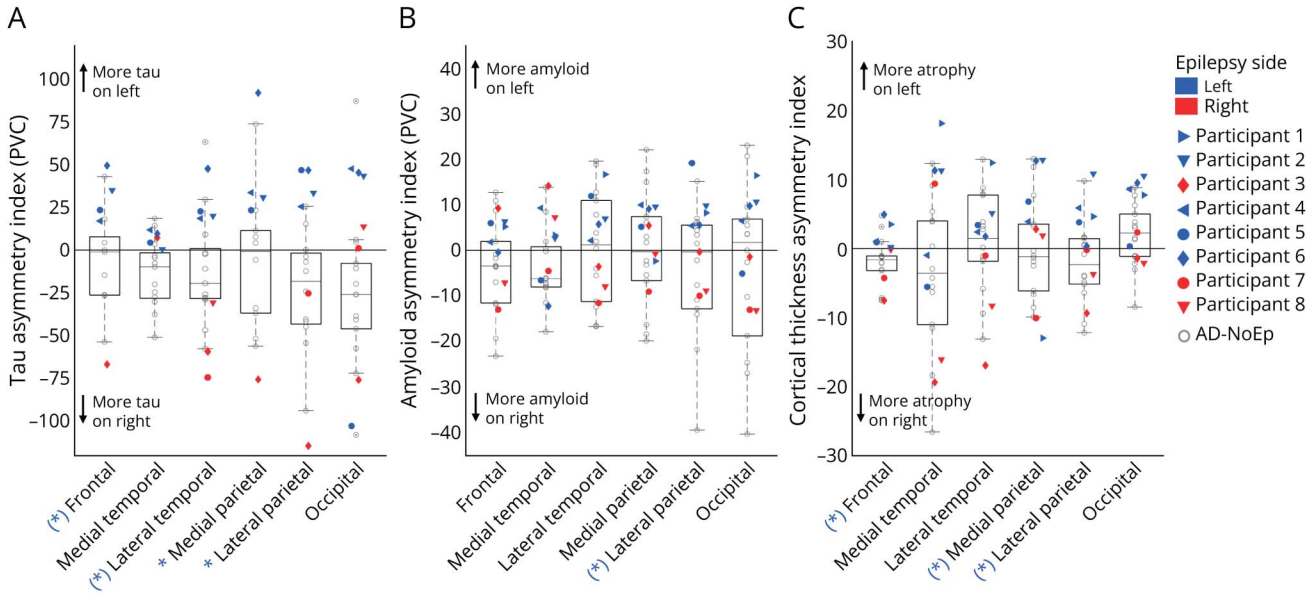

AIs were calculated with respect to the left hemisphere across 6 large brain regions, for (A) tau deposition, (B) amyloid deposition, and (C) cortical atrophy. A positive AI indicates greater tau deposition, amyloid deposition, or cortical atrophy in the left hemisphere while a negative AI indicates greater tau deposition, amyloid deposition, or cortical atrophy in the right hemisphere. Box-and-whisker plots are shown for the AD-NoEp group, with values for each AD-NoEp participant plotted as open black circles. AD-Ep participants are plotted using colored markers, based on whether their seizures arose from the left (blue) or right (red) hemisphere. AIs for tau and amyloid were calculated using partial volume–corrected SUVR and DVR values, respectively. AD-Ep participant 1 was excluded from the tau analysis because their tau PET imaging was performed using FTP, rather than with MK-6240. Blue asterisks denote ROIs in which the AI for AD-Ep participants with left-sided seizures was significantly greater than for AD-NoEp (FDR-corrected p value < 0.025), whereas blue asterisks in parentheses indicate trends toward significance. AI = asymmetry index; DVR = distribution volume ratio; SUVR = standardized uptake value ratio.

Findings for amyloid and atrophy asymmetry between AD-Ep and AD-NoEp groups were less striking. For amyloid, AD-Ep participants with left-sided epilepsy showed a trend toward greater left-sided asymmetry in the lateral parietal region (p = 0.0583, r = 0.52) compared with AD-NoEp. For atrophy, AD-Ep participants with left-sided epilepsy showed a trends toward greater left-sided asymmetry in the frontal (p = 0.0346, r = 0.49), medial parietal (p = 0.0346, r = 0.49), and lateral parietal (p = 0.0346, r = 0.49) regions, compared with AD-NoEp.

We also assessed relationships between tau asymmetry, amyloid asymmetry, and atrophy asymmetry, across different brain regions, for AD-Ep and AD-NoEp groups (eAppendix and eFigures 4 and 5). In the AD-NoEp group, tau asymmetry was positively correlated with amyloid asymmetry and atrophy asymmetry, in multiple brain regions. With the limitation of low sample size, these relationships seemed to be largely similar in the AD-Ep group.

Comparison of Tau Burden, Amyloid Burden, and Cortical Thickness in AD-Ep vs AD-NoEp

To better understand the observed differences in asymmetry between AD-Ep and AD-NoEp, we next compared tau burden, amyloid burden, and cortical thickness between AD-Ep and AD-NoEp groups (Figure 4). For tau burden (Figure 4A), most AD-Ep participants had tau SUVRs in the epileptogenic hemisphere that were in or above the upper range of the AD-NoEp distribution. For AD-Ep participants with left-sided epilepsy, there were trends for increased tau burden in the medial temporal (p = 0.095, r = 0.34), lateral temporal (p = 0.079, r = 0.44), medial parietal (p = 0.095, r = 0.36), lateral parietal (p = 0.079, r = 0.44), and occipital (p = 0.079, r = 0.44) regions of the epileptogenic hemisphere, compared with AD-NoEp. There were no significant or trending group differences in tau burden in the non-epileptogenic hemisphere. Two AD-Ep participants with right-sided epilepsy (participants 7 and 8) were outliers because they both had subthreshold or near-threshold tau SUVRs in most brain regions, except for the epileptogenic lateral temporal region, where their tau burden was in the low-mid range of the AD-NoEp distribution. These findings could be due to both participants being in earlier pathologic stages of AD, as their amyloid burden was also lower compared with other AD-Ep participants, although within the norm for AD-NoEp (Figure 4B).

For amyloid burden (Figure 4B), AD-Ep participants with left-sided epilepsy had amyloid deposition that was significantly (or nearly significantly) higher compared with AD-NoEp, for regions in both the epileptogenic hemisphere (frontal (p = 0.025, r = 0.5), medial temporal (p = 0.0036, r = 0.67), lateral temporal (p = 0.0254, r = 0.5), medial parietal (p = 0.0254, r = 0.46, and lateral parietal (p = 0.052, r = 0.39)) and the

Figure 4 Comparison of Tau Burden, Amyloid Burden, and Cortical Thickness Between AD-Ep and AD-NoEp Groups

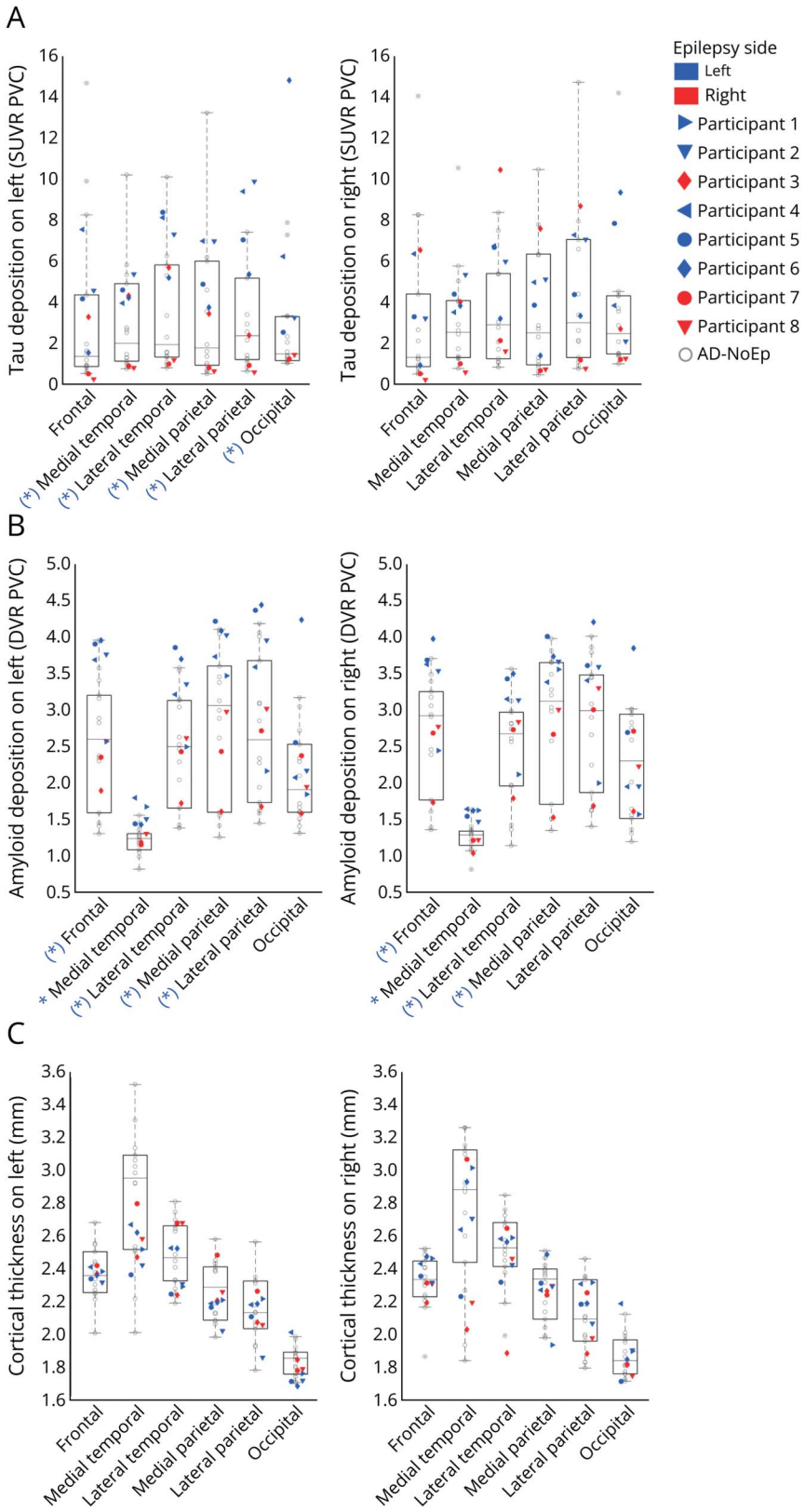

(A) Tau burden. MK-6240 SUVRs (PVC) were averaged across 6 large brain regions in the left hemisphere (left) and right hemisphere (right). The AD-NoEp distribution is shown as a box-and-whisker plot, with values for AD-NoEp participants plotted as open black circles. Values for AD-Ep participants are plotted using colored markers, based on whether their seizures arose from the left (blue) or right (red) hemisphere. Participant 1 was excluded from the tau analysis because their tau PET imaging was performed using FTP, rather than with MK-6240. (B) Amyloid burden. Format is similar to (A) but uses PIB DVRs (PVC). (C) Cortical thickness. Format is similar to (A). Blue asterisks represent statistically significant differences between AD-Ep participants with left-sided epilepsy and the AD-NoEp group (FDR-corrected p value < 0.025). Blue asterisks in parentheses represent trending differences between these groups. DVR = distribution volume ratio; PIB = Pittsburgh Compound B; PVC = partial volume correction; SUVR = standardized uptake value ratio.

nonepileptogenic hemisphere (frontal (p = 0.033, r = 0.48), medial temporal (p = 0.0062, r = 0.65), lateral temporal (p = 0.033, r = 0.46), and medial parietal (p = 0.033, r = 0.46)). AD-Ep participants with right-sided epilepsy did not show higher amyloid burden in either hemisphere compared with AD-NoEp. It is unclear whether this finding is specific to right-sided epilepsy

in AD or due to our sample of participants with right-sided epilepsy being in earlier disease stages.

For cortical thickness (Figure 4C), we did not find any significant or trending group differences between AD-Ep and AD-NoEp groups, for regions in either the epileptogenic or nonepileptogenic hemisphere.

Relationships Between Epilepsy Characteristics and Tau and Amyloid Burden Deposition and Asymmetry

Finally, we examined how epilepsy characteristics were associated with tau and amyloid burden and asymmetry. We found no significant associations between epilepsy duration (latency between first seizure and PET imaging) and global or regional tau or amyloid burden. There was also no significant association between epilepsy duration and tau or amyloid AI. We also examined whether the burden of epileptiform abnormalities on scalp EEG was related to amyloid or tau burden or asymmetry. We stratified AD-Ep participants based on whether they had epileptiform discharges on scalp EEG. We found no association between scalp EEG epileptiform abnormalities and amyloid or tau burden or AI.

Discussion

Individuals with AD who develop epilepsy often have lateralized epileptiform abnormalities,[12-14,26] raising the question of why epilepsy arising in AD is asymmetric while AD pathology is often assumed to be symmetric. In this study of 8 individuals with early clinical stages of AD who developed late-onset focal epilepsy, we found greater tau deposition, amyloid deposition, and cortical atrophy within the epileptogenic hemisphere. Asymmetrically deposited tau in the epileptogenic hemisphere was the most striking finding, whereas asymmetries in amyloid deposition and cortical atrophy were less pronounced. Compared with a control AD group without epilepsy, the AD-Ep group showed greater tau asymmetry, greater amyloid burden bilaterally, and greater tau burden within the epileptogenic hemisphere. Relationships between tau, amyloid, and atrophy asymmetry were similar between AD-Ep and AD-NoEp. We found no associations between duration of epilepsy or extent of epileptiform abnormalities with tau or amyloid burden or asymmetry.

Asymmetries in tau and, to a lesser extent, amyloid deposition in AD have recently begun to be recognized, largely because of PET imaging studies that allow assessment of the entire brain,[23,24,27,28] as opposed to postmortem studies that typically sample only 1 hemisphere.[29] Asymmetric tau has primarily been described in atypical variants of AD such as logopenic variant primary progressive aphasia and posterior cortical atrophy.[23,30,31] Whether individuals with AD who develop epilepsy should be considered to have an atypical variant of AD warrants further consideration, although notably, all our participants had "typical" amnestic presentations of AD.

Recently, a data-driven approach was applied to a large sample of tau PET images from individuals with AD, to identify spatiotemporal patterns of tau progression in AD.[28] Four distinct tau trajectories were found, including a "lateral temporal" subtype, characterized by highly asymmetric cortical tau pathology involving the lateral temporoparietal regions. The "lateral temporal" subtype comprised 20% of the study population and was associated with worse global cognition and faster rate of cognitive decline, compared with other tau subtypes. Another group found that asymmetric cortical tau deposition in AD was associated with earlier age at onset and faster decline.[32] Asymmetric patterns of cortical tau deposition also occur in preclinical stages of AD, comprising 9% of cases.[24] Given the highly asymmetric cortical tau pathology seen in AD-Ep and previous work demonstrating that epilepsy in AD is associated with earlier age at onset of cognitive decline, greater cognitive impairment, and more aggressive disease course,[4] we hypothesize that development of epilepsy in preclinical and early clinical stages of AD[12,33] is associated with the "lateral temporal" tau subtype.

Amyloid asymmetry in AD has been less well characterized than tau, although some studies have reported asymmetric amyloid deposition in preclinical and clinical stages of AD.[27,34,35] Of interest, asymmetries in amyloid deposition have also been observed in genetic mouse models of AD using PET imaging, with strong asymmetries seen in 30% of these mice.[36] Whether amyloid asymmetry is associated with epileptiform spiking or seizures in these mice is unknown.

Whether lateralized AD pathology gives rise to focal epilepsy, or focal hyperexcitability drives lateralized accumulation of AD pathology, or a common mechanism drives both focal hyperexcitability and lateralized pathology in AD, is unclear. Our study offers some potentially important insights. First, we found that amyloid burden was significantly higher in AD-Ep compared with AD-NoEp and that this difference was strongest in the medial temporal region, though also seen in the frontal, lateral temporal, and medial parietal regions. One possibility, given the feed-forward mechanism that directly links soluble amyloid with neuronal hyperactivity,[5,6,37] is that high amyloid burden within the medial temporal lobe could precipitate local neuronal hyperexcitability, increasing susceptibility to medial temporal lobe seizures. Another possibility is that high amyloid burden in the neocortex could also drive medial temporal lobe hyperexcitability, through long-range network effects. A recent study found that high neocortical amyloid burden drives default mode network hyperexcitability, which, in turn, drives hyperexcitability of the medial temporal lobe and early accumulation of entorhinal tau.[38] We also found an asymmetry in neocortical amyloid deposition in AD-Ep, which might account for development of unilateral medial temporal lobe hyperexcitability. While this observed amyloid asymmetry was subtle, it is plausible that the magnitude of asymmetry was higher in earlier

stages of the disease because previous studies have shown that amyloid deposition may be most asymmetric in preclinical and prodromal stages of AD and then later become more symmetric.[34,35]

We did not find significant tau asymmetry in the medial temporal region in AD-Ep, nor did we find an increase in tau burden specific to the epileptogenic medial temporal lobe. Therefore, there is little evidence to suggest that medial temporal tau drives epilepsy in AD. However, it is possible that medial temporal tau could have been asymmetric earlier in the disease process, leading to asymmetric neocortical tau deposition, before saturating and becoming more symmetric by the time PET imaging was performed.

Of interest, we found that tau asymmetry in AD-Ep was widespread throughout neocortical regions and similar in magnitude across the frontal, lateral temporal, medial parietal, and lateral parietal regions, with increased tau throughout the epileptogenic hemisphere. AD-Ep participants had greater neocortical tau asymmetry compared with AD-NoEp, and several AD-Ep participants also had a higher tau burden in the epileptogenic hemisphere, compared with AD-NoEp. This widespread tau deposition could be consistent with the cascading network failure model of AD,[39,40] which posits that an initial local network failure (e.g., from unilateral medial temporal lobe hyperexcitability) triggers system-wide brain network compensatory changes (including changes in the default mode network) that later become overwhelmed as amyloid deposition saturates, resulting in decompensation of the initial failed network and rapid, widespread tau deposition throughout connected regions of the failed network. As studies in animal models of AD and epilepsy have demonstrated that tau is pro-epileptogenic,[41-45] it is possible that focal seizures could emerge in the context of this rapid, lateralized tau deposition. Of note, most AD-Ep participants developed clinical seizures in the same year that they presented with cognitive decline, which is consistent with the idea that changes in tau, rather than amyloid, may be more closely related to development of seizures in these participants. While there were subtle increases in cortical atrophy within the epileptogenic hemisphere, we did not find significant differences in cortical atrophy between AD-Ep and AD-NoEp groups. Thus, it is unlikely that neurodegeneration drives the development of epilepsy in AD.

With the major caveats of low sample size, cross-sectional design, and other unknown factors, we did not find compelling evidence that epilepsy drives lateralized AD pathology. Epilepsy duration was not significantly associated with amyloid or tau burden or asymmetry, although network hyperexcitability likely preceded development of epilepsy and the duration of this hyperexcitability is unknown. The presence of scalp EEG epileptiform abnormalities was also not significantly associated with amyloid or tau burden or asymmetry, although scalp EEG provides a poor proxy for medial temporal lobe epileptiform abnormalities.[14] Longitudinal studies are clearly needed to assess the relationship between focal seizures and epileptiform activity and subsequent changes in amyloid and tau deposition and cortical atrophy.

The strengths of this study include a well-characterized clinical cohort with detailed information on the cognitive, neurophysiologic, and neuroimaging aspects of each case. Limitations include its small sample size and cross-sectional design. Moreover, our study population was entirely White, non-Hispanic, and highly educated. These limitations underscore the need for larger, longitudinal studies with a more diverse study population.

Altogether, our study reveals a spatial association between focal epilepsy and asymmetries in tau deposition, amyloid deposition, and cortical atrophy in early clinical stages of AD. Historically, individuals with AD and epilepsy were excluded from almost all observational studies and clinical trials in AD. Yet, studying these individuals can provide unique insights into our understanding of the clinical and pathologic heterogeneity of AD, with the possibility of improving disease prognostication and guiding the development of novel targeted therapies aimed toward specific AD subtypes.

Study Funding

American Academy of Neurology Institute (ADL), National Institutes of Health (NIH K23NS101037; R21AG064413; ADL), Alzheimer's Association (AARGD-22-974081; ADL). While this article was funded by the American Academy of Neurology, the findings and conclusions in this article are those of the authors and do not necessarily represent the official position of the American Academy of Neurology.

Disclosure

The authors report no relevant disclosures. Go to Neurology.org/N for full disclosures.

Publication History

Received by *Neurology* February 27, 2024. Accepted in final form August 22, 2024. Submitted and externally peer reviewed. The handling editor was Associate Editor Barbara Jobst, MD, PhD, FAAN.

Appendix Authors

Name	Location	Contribution
Alice D. Lam, MD, PhD	Department of Neurology, Massachusetts General Hospital; Harvard Medical School	Drafting/revision of the manuscript for content, including medical writing for content; major role in the acquisition of data; study concept or design; analysis or interpretation of data
Emma G. Thibault, BS	Department of Radiology, Massachusetts General Hospital	Drafting/revision of the manuscript for content, including medical writing for content; analysis or interpretation of data

Continued

Appendix *(continued)*

Name	Location	Contribution
Danielle V. Mayblyum, BS	Department of Radiology, Massachusetts General Hospital	Drafting/revision of the manuscript for content, including medical writing for content; analysis or interpretation of data
Stephanie Hsieh, BS	Department of Neurology, Massachusetts General Hospital	Drafting/revision of the manuscript for content, including medical writing for content; analysis or interpretation of data
Kyle R. Pellerin, BA	Department of Neurology, Massachusetts General Hospital	Major role in the acquisition of data
Eliezer J. Sternberg, MD	Department of Neurology, Milford Regional Medical Center	Drafting/revision of the manuscript for content, including medical writing for content; major role in the acquisition of data
Anand Viswanathan, MD, PhD	Department of Neurology, Massachusetts General Hospital; Harvard Medical School	Drafting/revision of the manuscript for content, including medical writing for content; major role in the acquisition of data
Stephanie Buss, MD	Harvard Medical School; Department of Neurology, Beth Israel Deaconess Medical Center	Drafting/revision of the manuscript for content, including medical writing for content
Rani A. Sarkis, MD, MSc	Harvard Medical School, Department of Neurology, Brigham and Women's Hospital	Drafting/revision of the manuscript for content, including medical writing for content; analysis or interpretation of data
Heidi I.L. Jacobs, PhD	Harvard Medical School; Department of Radiology, Massachusetts General Hospital	Drafting/revision of the manuscript for content, including medical writing for content; study concept or design; analysis or interpretation of data
Keith A. Johnson, MD	Department of Neurology, Massachusetts General Hospital; Harvard Medical School; Department of Radiology, Massachusetts General Hospital	Study concept or design; analysis or interpretation of data
Reisa A. Sperling, MD	Harvard Medical School; Department of Neurology, Brigham and Women's Hospital	Drafting/revision of the manuscript for content, including medical writing for content; study concept or design; analysis or interpretation of data

References

1. Harris SS, Wolf F, De Strooper B, Busche MA. Tipping the scales: peptide-dependent dysregulation of neural circuit dynamics in Alzheimer's disease. *Neuron.* 2020;107(3):417-435. doi:10.1016/j.neuron.2020.06.005
2. Palop JJ, Mucke L. Network abnormalities and interneuron dysfunction in Alzheimer disease. *Nat Rev Neurosci.* 2016;17(12):777-792. doi:10.1038/nrn.2016.141
3. Vossel KA, Tartaglia MC, Nygaard HB, Zeman AZ, Miller BL. Epileptic activity in Alzheimer's disease: causes and clinical relevance. *Lancet Neurol.* 2017;16(4):311-322. doi:10.1016/S1474-4422(17)30044-3
4. Vöglein J, Ricard I, Noachtar S, et al. Seizures in Alzheimer's disease are highly recurrent and associated with a poor disease course. *J Neurol.* 2020;267(10):2941-2948. doi:10.1007/s00415-020-09937-7
5. Busche MA, Chen X, Henning HA, et al. Critical role of soluble amyloid-β for early hippocampal hyperactivity in a mouse model of Alzheimer's disease. *Proc Natl Acad Sci U S A.* 2012;109(22):8740-8745. doi:10.1073/pnas.1206171109
6. Bero AW, Yan P, Roh JH, et al. Neuronal activity regulates the regional vulnerability to amyloid-β deposition. *Nat Neurosci.* 2011;14(6):750-756. doi:10.1038/nn.2801
7. Pooler AM, Phillips EC, Lau DHW, Noble W, Hanger DP. Physiological release of endogenous tau is stimulated by neuronal activity. *EMBO Rep.* 2013;14(4):389-394. doi:10.1038/embor.2013.15
8. Wu JW, Hussaini SA, Bastille IM, et al. Neuronal activity enhances tau propagation and tau pathology in vivo. *Nat Neurosci.* 2016;19(8):1085-1092. doi:10.1038/nn.4328
9. Jacobs HIL, Hedden T, Schultz AP, et al. Structural tract alterations predict downstream tau accumulation in amyloid-positive older individuals. *Nat Neurosci.* 2018;21(3):424-431. doi:10.1038/s41593-018-0070-z
10. Franzmeier N, Neitzel J, Rubinski A, et al. Functional brain architecture is associated with the rate of tau accumulation in Alzheimer's disease. *Nat Commun.* 2020;11(1):347. doi:10.1038/s41467-019-14159-1
11. Ossenkoppele R, Iaccarino L, Schonhaut DR, et al. Tau covariance patterns in Alzheimer's disease patients match intrinsic connectivity networks in the healthy brain. *Neuroimage Clin.* 2019;23:101848. doi:10.1016/j.nicl.2019.101848
12. Vossel KA, Beagle AJ, Rabinovici GD, et al. Seizures and epileptiform activity in the early stages of Alzheimer disease. *JAMA Neurol.* 2013;70(9):1158-1166. doi:10.1001/jamaneurol.2013.136
13. Lam AD, Sarkis RA, Pellerin KR, et al. Association of epileptiform abnormalities and seizures in Alzheimer disease. *Neurology.* 2020;95(16):e2259-e2270. doi:10.1212/wnl.0000000000010612
14. Lam AD, Deck G, Goldman A, Eskandar EN, Noebels J, Cole AJ. Silent hippocampal seizures and spikes identified by foramen ovale electrodes in Alzheimer's disease. *Nat Med.* 2017;23(6):678-680. doi:10.1038/nm.4330
15. Albert MS, DeKosky ST, Dickson D, et al. The diagnosis of mild cognitive impairment due to Alzheimer's disease: recommendations from the National Institute on Aging-Alzheimer's Association workgroups on diagnostic guidelines for Alzheimer's disease. *Alzheimers Dement.* 2011;7(3):270-279. doi:10.1016/j.jalz.2011.03.008
16. McKhann GM, Knopman DS, Chertkow H, et al. The diagnosis of dementia due to Alzheimer's disease: recommendations from the National Institute on Aging-Alzheimer's Association workgroups on diagnostic guidelines for Alzheimer's disease. *Alzheimers Dement.* 2011;7(3):263-269. doi:10.1016/j.jalz.2011.03.005
17. Fisher RS, Acevedo C, Arzimanoglou A, et al. ILAE official report: a practical clinical definition of epilepsy. *Epilepsia.* 2014;55(4):475-482. doi:10.1111/epi.12550
18. FreeSurfer Software Suite. *Laboratories for Computational Neuroimaging at the Athinoula A. Martinos Center for Biomedical Imaging.* Accessed May 7, 2024. surfer.nmr.mgh.harvard.edu/
19. Dale AM, Fischl B, Sereno MI. Cortical surface-based analysis. I. Segmentation and surface reconstruction. *Neuroimage.* 1999;9(2):179-194. doi:10.1006/nimg.1998.0395
20. Desikan RS, Ségonne F, Fischl B, et al. An automated labeling system for subdividing the human cerebral cortex on MRI scans into gyral based regions of interest. *Neuroimage.* 2006;31(3):968-980. doi:10.1016/j.neuroimage.2006.01.021
21. Logan J, Fowler JS, Volkow ND, et al. Graphical analysis of reversible radioligand binding from time-activity measurements applied to [N-11C-Methyl]-(-)-cocaine PET studies in human subjects. *J Cereb Blood flow Metab.* 1990;10(5):740-747. doi:10.1038/jcbfm.1990.127
22. Hedden T, Van Dijk KRA, Becker JA, et al. Disruption of functional connectivity in clinically normal older adults harboring amyloid burden. *J Neurosci.* 2009;29(40):12686-12694. doi:10.1523/JNEUROSCI.3189-09.2009
23. Ossenkoppele R, Schonhaut DR, Schöll M, et al. Tau PET patterns mirror clinical and neuroanatomical variability in Alzheimer's disease. *Brain.* 2016;139(Pt 5):1551-1567. doi:10.1093/brain/aww027
24. Young CB, Winer JR, Younes K, et al. Divergent cortical tau positron emission tomography patterns among patients with preclinical Alzheimer disease. *JAMA Neurol.* 2022;79(6):592-603. doi:10.1001/jamaneurol.2022.0676
25. Vogel JW, Iturria-Medina Y, Strandberg OT, et al. Spread of pathological tau proteins through communicating neurons in human Alzheimer's disease. *Nat Commun.* 2020;11(1):2612. doi:10.1038/s41467-020-15701-2
26. Vossel KA, Ranasinghe KG, Beagle AJ, et al. Incidence and impact of subclinical epileptiform activity in Alzheimer's disease. *Ann Neurol.* 2016;80(6):858-870. doi:10.1002/ana.24794
27. Frings L, Hellwig S, Spehl TS, et al. Asymmetries of amyloid-β burden and neuronal dysfunction are positively correlated in Alzheimer's disease. *Brain.* 2015;138(Pt 10):3089-3099. doi:10.1093/brain/awv229
28. Vogel JW, Young AL, Oxtoby NP, et al. Four distinct trajectories of tau deposition identified in Alzheimer's disease. *Nat Med.* 2021;27(5):871-881. doi:10.1038/s41591-021-01309-6
29. King A, Bodi I, Nolan M, Troakes C, Al-Sarraj S. Assessment of the degree of asymmetry of pathological features in neurodegenerative diseases. What is the significance for brain banks? *J Neural Transm (Vienna).* 2015;122(10):1499-1508. doi:10.1007/s00702-015-1410-8
30. Xia C, Makaretz SJ, Caso C, et al. Association of in vivo [18F]AV-1451 tau PET imaging results with cortical atrophy and symptoms in typical and atypical Alzheimer disease. *JAMA Neurol.* 2017;74(4):427-436. doi:10.1001/jamaneurol.2016.5755
31. Tetzloff KA, Graff-Radford J, Martin PR, et al. Regional distribution, asymmetry, and clinical correlates of tau uptake on [18F]AV-1451 PET in atypical Alzheimer's disease. *J Alzheimers Dis.* 2018;62(4):1713-1724. doi:10.3233/JAD-170740
32. Lu J, Zhang Z, Wu P, et al. The heterogeneity of asymmetric tau distribution is associated with an early age at onset and poor prognosis in Alzheimer's disease. *Neuroimage Clin.* 2023;38:103416. doi:10.1016/j.nicl.2023.103416

33. Sarkis RA, Dickerson BC, Cole AJ, Chemali ZN. Clinical and neurophysiologic characteristics of unprovoked seizures in patients diagnosed with dementia. *J Neuropsychiatry Clin Neurosci.* 2016;28(1):56-61. doi:10.1176/appi.neuropsych.15060143
34. Yoon HJ, Kim BS, Jeong JH, Kim GH, Park HK, Chun MY. Asymmetric amyloid deposition as an early sign of progression in mild cognitive impairment due to Alzheimer disease. *Clin Nucl Med.* 2021;46(7):527-531. doi:10.1097/RLU.0000000000003662
35. Kjeldsen PL, Parbo P, Hansen KV, et al. Asymmetric amyloid deposition in preclinical Alzheimer's disease: a PET study. *Aging Brain.* 2022;2:100048. doi:10.1016/j.nbas.2022.100048
36. Sacher C, Blume T, Beyer L, et al. Asymmetry of fibrillar plaque burden in amyloid mouse models. *J Nucl Med.* 2020;61(12):1825-1831. doi:10.2967/jnumed.120.242750
37. Cirrito JR, Yamada KA, Finn MB, et al. Synaptic activity regulates interstitial fluid amyloid-beta levels in vivo. *Neuron.* 2005;48(6):913-922. doi:10.1016/j.neuron.2005.10.028
38. Giorgio J, Adams JN, Maass A, Jagust WJ, Breakspear M. Amyloid induced hyperexcitability in default mode network drives medial temporal hyperactivity and early tau accumulation. *Neuron*. 2024;112(4):676-686.e4. doi:10.1016/j.neuron.2023.11.014
39. Jones DT, Knopman DS, Gunter JL, et al. Cascading network failure across the Alzheimer's disease spectrum. *Brain.* 2016;139(Pt 2):547-562. doi:10.1093/brain/awv338
40. Jones DT, Graff-Radford J, Lowe VJ, et al. Tau, amyloid, and cascading network failure across the Alzheimer's disease spectrum. *Cortex*. 2017;97:143-159. doi:10.1016/j.cortex.2017.09.018
41. Gomez-Murcia V, Sandau U, Ferry B, et al. Hyperexcitability and seizures in the THY-Tau22 mouse model of tauopathy. *Neurobiol Aging.* 2020;94:265-270. doi:10.1016/j.neurobiolaging.2020.06.004
42. Chang CW, Evans MD, Yu X, Yu GQ, Mucke L. Tau reduction affects excitatory and inhibitory neurons differently, reduces excitation/inhibition ratios, and counteracts network hypersynchrony. *Cell Rep.* 2021;37(3):109855. doi:10.1016/j.celrep.2021.109855
43. Holth JK, Bomben VC, Reed JG, et al. Tau loss attenuates neuronal network hyperexcitability in mouse and drosophila genetic models of epilepsy. *J Neurosci.* 2013;33(4):1651-1659. doi:10.1523/JNEUROSCI.3191-12.2013
44. Gheyara AL, Ponnusamy R, Djukic B, et al. Tau reduction prevents disease in a mouse model of Dravet syndrome. *Ann Neurol.* 2014;76(3):443-456. doi:10.1002/ana.24230
45. DeVos SL, Goncharoff DK, Chen G, et al. Antisense reduction of tau in adult mice protects against seizures. *J Neurosci.* 2013;33(31):12887-12897. doi:10.1523/JNEUROSCI.2107-13.2013